



ERK/RSK-mediated phosphorylation of Y-box binding protein-1 aggravates diabetic cardiomyopathy by suppressing its interaction with deubiquitinase OTUB1

Received for publication, September 14, 2021, and in revised form, April 22, 2022. Published, Papers in Press, April 28, 2022.

<https://doi.org/10.1016/j.jbc.2022.101989>

Xiaodan Zhong (钟晓丹)^{1,2}, Tao Wang (王涛)^{1,3}, Wenjun Zhang (张文君)^{1,2}, Mengwen Wang (王孟文)^{1,2}, Yang Xie (谢阳)^{1,2}, Lei Dai (代磊)^{1,2}, Xingwei He (贺行巍)^{1,2}, Thati Madhusudhan⁴, Hesong Zeng (曾和松)^{1,2,*}, and Hongjie Wang (王洪杰)^{1,2,*}

From the ¹Division of Cardiology, Tongji Hospital, Tongji Medical College, Huazhong University of Science and Technology, Wuhan, PR China; ²Hubei Key Laboratory of Genetics and Molecular Mechanisms of Cardiological Disorders, Wuhan, PR China; ³Department of Cardiology, Affiliated Hospital of Weifang Medical University, Weifang, Shandong, PR China; ⁴Center for Thrombosis and Hemostasis, University Medical Center Mainz, Mainz, Germany

Edited by George DeMartino

Diabetic cardiomyopathy (DCM) is a major complication of diabetes, but its underlying mechanisms still remain unclear. The multifunctional protein Y-box binding protein-1 (YB-1) plays an important role in cardiac pathogenesis by regulating cardiac apoptosis, cardiac fibrosis, and pathological remodeling, whereas its role in chronic DCM requires further investigation. Here, we report that the phosphorylation of YB-1 at serine102 (S102) was markedly elevated in streptozotocin-induced diabetic mouse hearts and in high glucose-treated cardiomyocytes, whereas total YB-1 protein levels were significantly reduced. Coimmunoprecipitation experiments showed that YB-1 interacts with the deubiquitinase otubain-1, but hyperglycemia-induced phosphorylation of YB-1 at S102 diminished this homeostatic interaction, resulting in ubiquitination and degradation of YB-1. Mechanistically, the high glucose-induced phosphorylation of YB-1 at S102 is dependent on the upstream extracellular signal-regulated kinase (ERK)/Ras/mitogen-activated protein kinase (p90 ribosomal S6 kinase [RSK]) signaling pathway. Accordingly, pharmacological inhibition of the ERK pathway using the upstream kinase inhibitor U0126 ameliorated features of DCM compared with vehicle-treated diabetic mice. We demonstrate that ERK inhibition with U0126 also suppressed the phosphorylation of the downstream RSK and YB-1 (S102), which stabilized the interaction between YB-1 and otubain-1 and thereby preserved YB-1 protein expression in diabetic hearts. Taken together, we propose that targeting the ERK/RSK/YB-1 pathway could be a potential therapeutic approach for treating DCM.

Diabetic cardiomyopathy (DCM) is defined as diabetes-associated cardiac dysfunction independent of coronary artery diseases or other confounding cardiovascular diseases (1, 2). DCM is characterized by structural and functional disorders, including cardiomyocyte hypertrophy, interstitial

fibrosis, microvascular rarefaction, and metabolic deregulation (3). Although intensive glucose control in diabetic patients reduced the incidence of coronary events, it generally had a neutral effect on cardiovascular mortality and sometimes resulted in exacerbation of heart failure (4, 5). Despite massive research in the past decade, there is no available therapy for DCM. This prompts us to further explore the novel potential molecular mechanism for deciphering this clinical conundrum.

Y-box binding protein-1 (YB-1) is a member of the highly conserved cold shock domain protein family with various biological functions, including regulation of transcription, translation, and mRNA splicing (6, 7). Post-translational modification (PTM) plays an important role in regulating the function of YB-1. Previous studies found that the phosphorylation of YB-1 at serine102 (S102) by AKT and p90 ribosomal S6 kinase (RSK) plays an important role in regulation of DNA transcription and RNA translation (8, 9). Our recent data showed that the coagulation protease activated protein C can modulate the ubiquitination of YB-1 by regulating the expression of deubiquitinase otubain-1 (OTUB1), which exerts cytoprotective effect in mouse models of renal ischemia reperfusion injury (10). Besides, it has been shown to play an important role in cardiac pathogenesis by regulating the cardiac apoptosis (11), cardiac fibrosis (12, 13), cardiac fetal gene expression, and pathological remodeling of the heart (14). Furthermore, YB-1 has been reported to regulate angiogenesis in various tumors (15, 16). Considering the involvement of YB-1 in DCM-related pathogenesis, we speculate that it could be a potential intracellular target in the occurrence and progression of DCM.

The ovarian tumor domain (OTU) deubiquitylating proteases OTUB1 and OTUB2 (OTU deubiquitinase, ubiquitin aldehyde binding 1 and 2) are representative members of the OTU subfamily of deubiquitinases. Deubiquitination critically regulates a multitude of important cellular processes, such as cell metabolism, differentiation, proliferation, signaling, and apoptosis (17, 18). Interestingly, OTUB1 preferentially induces cleavage of

* For correspondence: Hongjie Wang, hongjie.wang@tjh.tjmu.edu.cn; Hesong Zeng, zenghs@tjh.tjmu.edu.cn.

YB-1 phosphorylation aggravates DCM

lysine 48 (K48)-linked polyubiquitin chains over K63-linked polyubiquitin chains (19). The function of polyubiquitin chain is determined by the type of ubiquitin side-chain linkage. For example, K48 chain-attached proteins will be most probably directed for proteasomal degradation, whereas K63 chains often regulate lysosomal targeting and protein interactions (20). We recently demonstrated that the ischemia-reperfusion injury can impair the homeostatic interaction of YB-1 and OTUB1, which results in YB-1 K48 polyubiquitination and subsequent proteasome degradation in renal tubular cells (10). The critical role of YB-1 in cardiac pathogenesis and experimental models of ischemia-reperfusion injury prompted us to investigate its role in regulation of DCM.

In a mouse model of chronic insulinopenic diabetes induced by streptozotocin (STZ), persistent hyperglycemia promoted the proteasome-mediated degradation of YB-1 in diabetic heart tissue. Mechanistically, hyperglycemia impairs the homeostatic interaction between YB-1 and OTUB1, which results in enhanced YB-1 ubiquitination and subsequent proteasome degradation. Hyperglycemia induced the phosphorylation of YB-1 at S102, which diminishes the interaction between YB-1 and OTUB1. Pharmacological targeting of the upstream kinases extracellular signal-regulated kinase (ERK)1/2 and RSK inhibited the hyperglycemia-induced S102 phosphorylation of the YB-1 and restored YB-1 protein levels in cultured cardiomyocytes. In accordance with the aforementioned *in vitro* findings, inhibition of ERK pathway in mice with U0126 ameliorated DCM.

Results

YB-1 phosphorylation was elevated in DCM

To determine YB-1 regulation in DCM, we established diabetic mice model with STZ intraperitoneal injection (Fig. 1A). We observed that the ratio of heart weight to body weight was significantly higher in diabetic mice (Fig. 1B). Also, random blood glucose detected *via* tail vein was much higher in diabetic mice during the whole process (Fig. 1C). As shown in wheat germ agglutinin (WGA) and HE staining, we found that diabetic mice exhibited structural alterations in cardiomyocytes, characterized by swelling, hypertrophy, and disarrangement (Fig. 1, D–F). Next, we detected cardiac function with echocardiography and hemodynamic measures. Diabetic mice presented both diastolic and systolic dysfunction, with significantly lower ejection fraction, fraction shortening, maximal rates of decline of ventricular pressure, and maximal rates of rise of ventricular pressure (Fig. 1, G–K and Table 1). In addition, we found that the protein expression of hypertrophy markers, including atrial natriuretic peptide (ANP), brain natriuretic peptide (BNP), and β -myosin heavy chain (β -MHC), was increased in diabetic mice heart compared with controls (Fig. 1, L and M). These data indicate a well-established mouse model of DCM. Interestingly, while YB-1 was downregulated in the hearts of diabetic mice, its phosphorylation (S102) was significantly elevated (Figs. 1, N–P and S1). These data suggest that the phosphorylation of YB-1 might play a crucial role in preserving YB-1 expression.

YB-1 phosphorylation promoted YB-1 degradation through ubiquitination

To investigate the effect of high glucose on YB-1 phosphorylation in YB-1 expression regulation, phosphorylated YB-1 level was detected in H9c2 cells stimulated with 25 mM glucose at different time points. Consistent with the *ex vivo* data, as YB-1 protein expression decreased over time, its phosphorylation was upregulated (Fig. 2, A and B). Next, we detected the effect of high glucose on YB-1 ubiquitination and degradation. As shown, YB-1 ubiquitination was gradually increased with the incubated time of high glucose, suggesting that high glucose had the ability to promote YB-1 degradation *via* ubiquitination (Figs. 2, A–C and S2A). Also, the interaction between YB-1 and OTUB1 was diminished by high glucose treatment (Fig. 2D). The kinetics of phosphorylation and ubiquitination in high glucose-treated H9c2 cells prompted us to investigate the role of YB-1 phosphorylation in regulation of its degradation. Different mutants of YB-1 S102 site were employed to modulate activation (102D) or inactivation (102A) of YB-1 phosphorylation. The YB-1 mutant (102D) exacerbated the high glucose-induced ubiquitination of YB-1, whereas YB-1 mutant (102A) effectively inhibited YB-1 ubiquitination (Figs. 2E and S2B). Moreover, pretreatment with 102A mutant lentivirus, which abolished the ability of YB-1 to be phosphorylated, fostered the interaction between YB-1 and deubiquitinating enzyme OTUB1 (Fig. 2F). These results indicate that the phosphorylation regulates the stability of YB-1 by enhancing its degradation through OTUB1-dependent ubiquitination.

Blockade of RSK functionally inhibited YB-1 phosphorylation

To address the mechanisms of YB-1 phosphorylation, we investigated signaling pathways upstream of YB-1, which may control its phosphorylation, including upstream kinase AKT and RSK. The phosphorylation level of RSK was significantly elevated in diabetic mice heart (Fig. 3, A and B), whereas the phosphorylation of AKT was reduced (Fig. S4, A and B). In addition, high glucose stimulation induced a gradual elevation of RSK phosphorylation over time (Fig. S3, A and B), but AKT phosphorylation level showed an increase in the first 3 h followed by a reduction at later time points (Fig. S4, C and D). To understand the role of RSK and AKT in YB-1 phosphorylation, H9c2 cells incubated with high glucose were cotreated with corresponding pharmacological inhibitors. Protein expression and phosphorylation level were determined by Western blots. Surprisingly, pharmacological blockade of AKT, MK2206, failed to regulate high glucose-induced YB-1 phosphorylation level (Fig. S4, E and F), which indicated that YB-1 phosphorylation in DCM was not mediated by AKT pathway. As shown, pretreatment with the pharmacological inhibitor SL-0101 represented an obviously dose-dependent reduction of RSK phosphorylation (Fig. S3, C and D), and pretreatment with 100 μ M SL-0101 for 30 min significantly reduced phosphorylation level of YB-1 in H9c2 cells stimulated by high glucose (Fig. 3, C–E), indicating that RSK was the regulator of YB-1 phosphorylation in DCM. Moreover, SL-0101 restored the

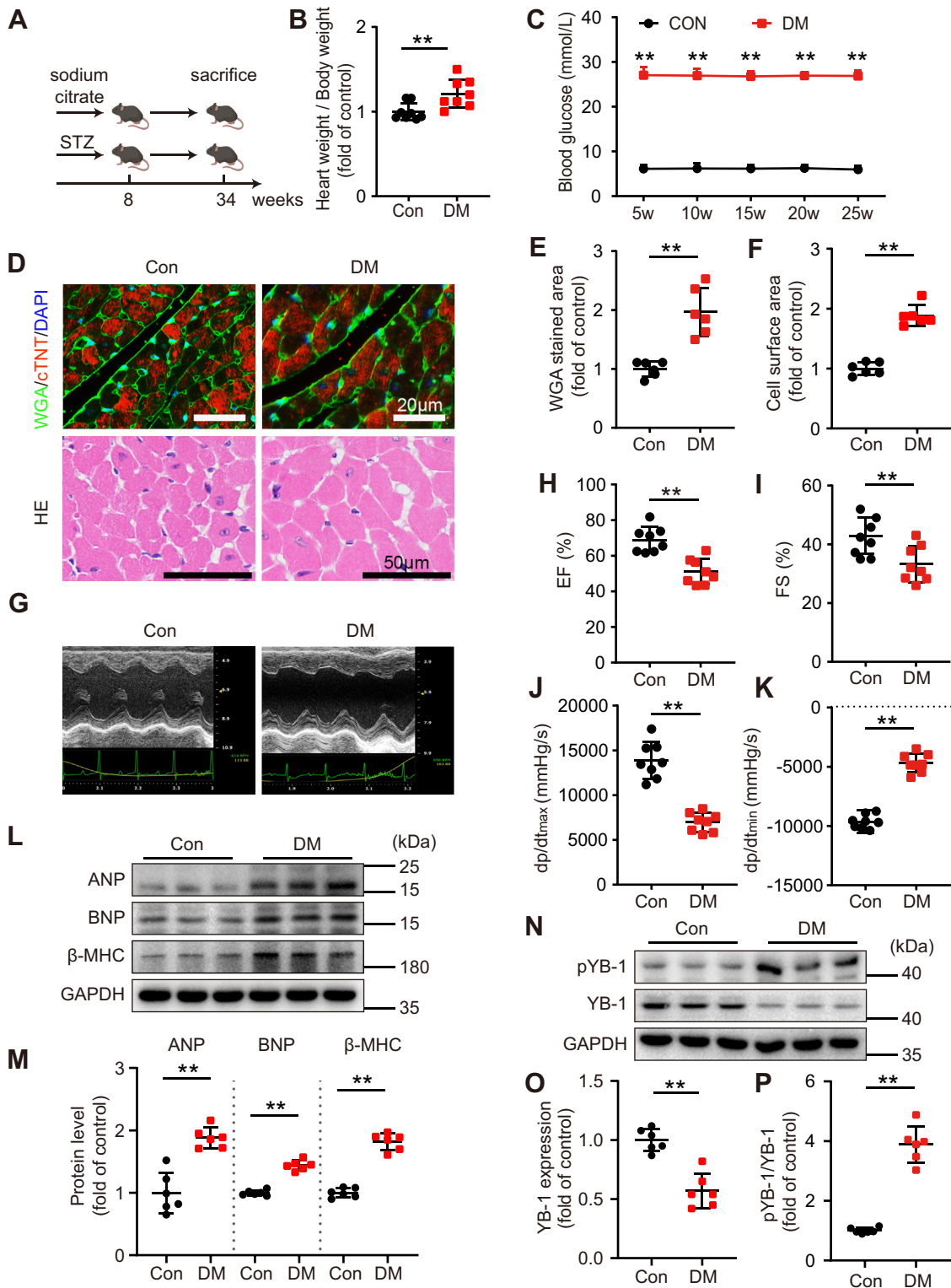


Figure 1. YB-1 phosphorylation was increased in diabetic mice heart. A, schematic diagram of animal experiment procedure. C57BL/6J male mice received 60 mg/kg STZ or sodium citrate for 5 days at the age of 8 weeks and sacrificed at 34 weeks. B, the ratios of heart weight to body weight in mice with diabetes mellitus compared with controls. C, blood glucose detected in different time points during the diabetic cardiomyopathy progression. D, representative images of transverse area of cardiomyocyte detected by WGA and HE staining. In WGA staining, green: WGA, red: cTNT, and blue: DAPI. The scale bar for WGA represents 20 μm, and the scale bar for HE represents 50 μm. E and F, histological analysis of WGA and HE staining. The areas of myocyte surface were calculated by Image-Pro Plus and standardized by control group. G, representative echocardiography images (M mode). H and I, echocardiography analysis of EF and FS. J and K, hemodynamic parameters measured by the Millar cardiac catheter system showing a reduction of cardiac function. L and M, representative immunoblotting images and analyzed scatter diagram showing the protein level of cardiac hypertrophy and dysfunction markers in heart tissue of mice with or without diabetes mellitus. N–P, immunoblotting images of phosphor-YB-1 (S102) and YB-1 protein expression. Analyzed data showed that the protein expression level of YB-1 was decreased, whereas its phosphorylation increased significantly. For all groups, n ≥ 6. Data are

YB-1 phosphorylation aggravates DCM

Table 1
Echocardiography result of mice in experiment 1

Item	Con	DM
Heart rate, bpm	498 ± 28.66	495 ± 30.72
Cardiac output, ml/min	25.74 ± 1.84	16.63 ± 3.56 ^a
LVAW; d, mm	0.65 ± 0.07	0.63 ± 0.06
LVAW; s, mm	1.04 ± 0.13	0.95 ± 0.10
LVID; d, mm	4.72 ± 0.22	4.24 ± 0.15 ^a
LVID; s, mm	3.58 ± 0.35	3.12 ± 0.24 ^a
LVPW; d, mm	0.64 ± 0.05	0.59 ± 0.05
LVPW; s, mm	0.98 ± 0.09	0.90 ± 0.12

Data are presented as mean ± SD, n = 8.

^a *p* < 0.01 versus Con.

Abbreviations: DM, diabetes mellitus; LVAW, left ventricular anterior wall; LVID, left ventricular internal dimension; LVPW, left ventricular posterior wall.

interaction between YB-1 and OTUB1 (Fig. 3F) and consequently ameliorated the ubiquitination modification of YB-1 (Fig. 3G).

ERK facilitated YB-1 phosphorylation through RSK

To further investigate the signaling pathway upstream of RSK, we next addressed the role of ERK, which was reported to regulate activation of RSK, in DCM. Our data showed a significantly elevated activation of ERK in heart tissue of diabetic mice represented by Western blot and immunohistochemical staining (Figs. 4, A and B and S5, A and B). Correspondingly, we observed a time-dependently increasing phosphorylation level of ERK in high glucose-stimulated H9c2 cells (Fig. S5, C and D). Because ERK activation was reported to be highly regulated by mitogen-activated protein kinase (MEK), MEK inhibitor U0126 was employed to treat high glucose-coincubated H9c2 cells. Our data showed that the treatment with U0126 significantly decreased the activation of ERK in a dose-dependent manner (Fig. S5, E and F). In addition, pretreatment with 10 μM U0126 significantly down-regulated phosphorylation of RSK and YB-1 (Fig. 4, C–F), demonstrating that ERK promoted YB-1 phosphorylation through RSK activation. To further explore the role of U0126 in regulating YB-1 protein stability, we performed coimmunoprecipitation (co-IP) and found that the treatment with U0126 restored the interaction between YB-1 and OTUB1 (Fig. 4G), thereby reducing YB-1 ubiquitination modification (Fig. 4H) and proteasome degradation.

U0126 alleviated DCM in vivo

Subsequently, diabetic mice were administrated with 1 mg/kg U0126 to verify its therapeutic effect on DCM *in vivo* (Fig. 5A). There were no significant differences in random blood glucose between diabetic mice with or without U0126 treatment (Fig. 5B). However, diabetic mice injected with U0126 showed a significant reduction in the ratio of heart weight to body weight, suggesting that U0126 potentially reversed cardiac hypertrophy (Fig. 5C), which was confirmed by WGA and HE

staining (Fig. 5, D–F). In addition, cardiac function of diabetic mice was also significantly improved by U0126 administration as analyzed by echocardiography and hemodynamic measures (Figs. 5, H and I, S6 and A and B and Table 2). We also observed that U0126 treatment downregulated the protein expression level of ANP, BNP, and β-MHC in diabetic mice heart (Figs. 5, J and S6, C and E). The phosphorylation levels of ERK, RSK, and YB-1 were highly reduced, and YB-1 protein expression was restored in U0126-treated diabetic mice heart, confirming the regulation effect of ERK/RSK/YB-1 pathway on YB-1 expression in DCM (Figs. 5, K and S6, F and H). Compared with diabetic mice, U0126 treatment showed a visible reduction in YB-1 K48-linked ubiquitination and a stable interaction with OTUB1 (Fig. 5, L and M). Taken together, our data identified that the ERK/RSK/YB-1 pathway plays a critical role in regulation of DCM (Fig. 6). Pharmacological targeting of ERK/RSK pathway with U0126 restores YB-1 function, which confers protective effect in mouse model of DCM.

Discussion

In the current study, we identify a novel mechanism by which phosphorylation of YB-1 on S102 could reduce its interaction with deubiquitinase OTUB1, which results in enhanced YB-1 ubiquitination and its subsequent degradation *via* proteasome in diabetic heart. While an MEK inhibitor U0126 could inhibit the phosphorylation of ERK1/2 and p90RSK and then YB-1, which could preserve the YB-1 protein level and ameliorate DCM.

YB-1 is an RNA-/DNA-binding multifunctional protein with biological activities ranging from transcription regulation, splicing, and translation, to the homeostasis of exosomal RNA (6, 7). Several PTMs have been reported to play an important role in modulating YB-1 function, among them phosphorylation at S102 is the most widely occurring PTM, which can regulate its intracellular distribution and subsequent signal transduction (21, 22). In congruent with our previous observations in mouse model of renal ischemia–reperfusion injury, the current study demonstrated that the YB-1 protein level decreased significantly in the diabetic heart (10). Surprisingly, we found that the protein levels of phosphorylated YB-1 at S102 increased almost fourfolds in the diabetic heart when compared with the nondiabetic control. Thus, we hypothesize that the phosphorylation of YB-1 could affect its protein stability. Indeed, high glucose treatment promoted YB-1 phosphorylation and its ubiquitination and subsequent proteasome degradation in cultured cardiomyocytes *in vitro*. Further experiments with constitutive active and inactive YB-1 mutants, S102D and S102A, proved our aforementioned hypothesis. However, besides S102, additional phosphorylation sites on YB-1 have been identified recently, including S165, S167, S174, S176, and S314, and the precise biological functions of these phosphorylation sites remain elusive (23, 24).

expressed as mean ± SD. ***p* < 0.01, Student's *t* test. cTNT, cardiac troponin T; DAPI, 4',6-diamidino-2-phenylindole; DM, diabetes mellitus; EF, ejection fraction; FS, fraction shortening; S102, serine102; STZ, streptozotocin; WGA, wheat germ agglutinin; YB-1, Y-box binding protein-1.

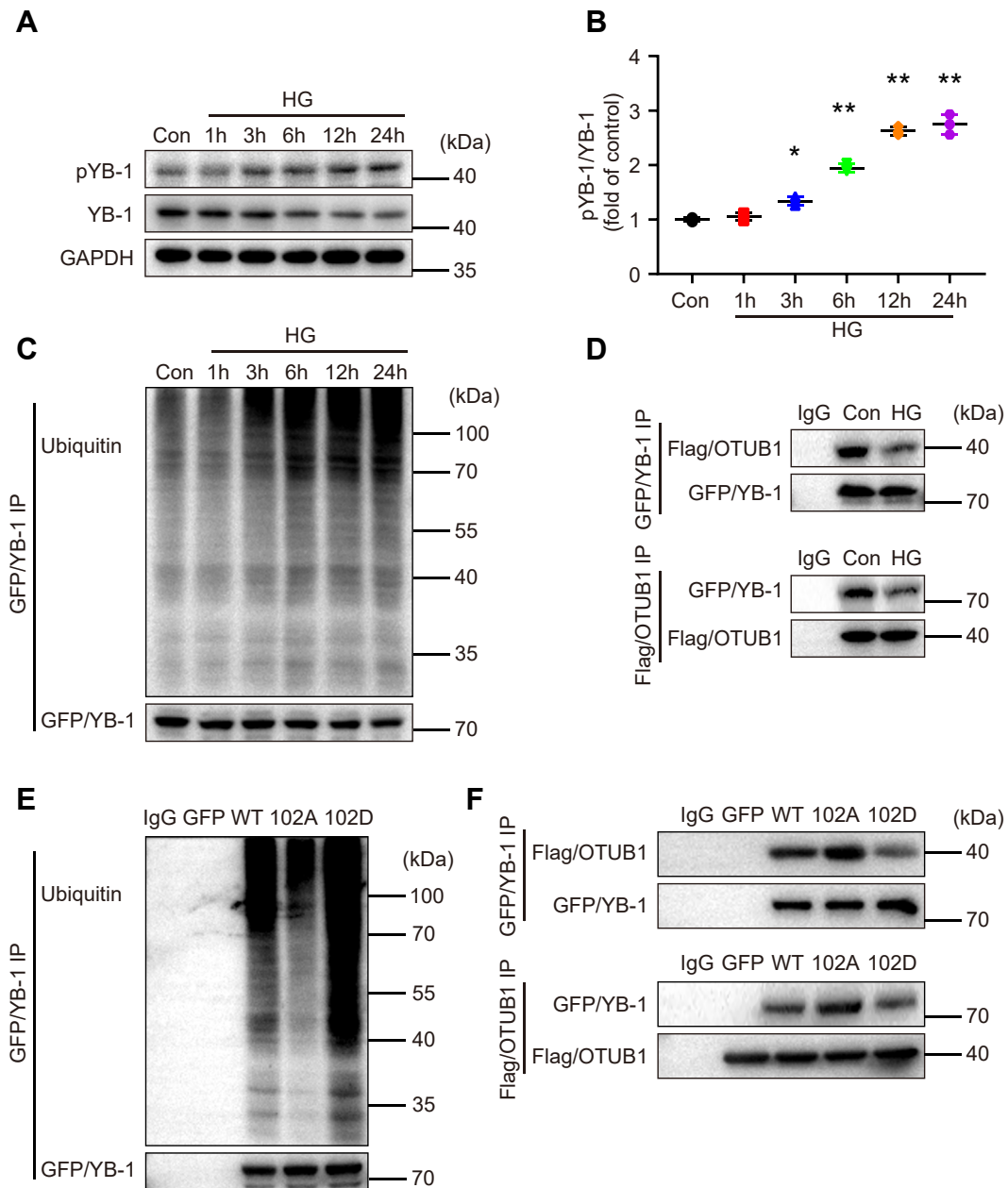


Figure 2. YB-1 phosphorylation induced YB-1 ubiquitination. A and B, Western blot images and analyzed data showed YB-1 protein expression and YB-1 phosphorylation (S102) level in H9c2 cells stimulated with high glucose (HG; 25 mM) at indicated time points. C, immunoprecipitation (IP) of YB-1 revealed a time-dependently elevated ubiquitination level of YB-1 protein in HG-challenged H9c2 cells. D, HG stimulation reduced the interaction between YB-1 and OTUB1. E, YB-1 phosphorylation aggravated YB-1 ubiquitination. H9c2 cells were infected with overexpressing YB-1 or mutant (102A/102D) lentivirus and stimulated by HG for 24 h. Mutant of 102A was used to imitate the dephosphorylation state, and mutant of 102D was used to imitate the continuous phosphorylation state. F, interaction between YB-1 and OTUB1 was suppressed by YB-1 phosphorylation. For all groups, n = 3. Analyzed data are expressed as mean ± SD. **p* < 0.05 and ***p* < 0.01, Student's *t* test. OTUB1, otubain-1; S102, serine102; YB-1, Y-box binding protein-1.

We and others have shown that the different types of PTM can mutually interact with each other and coordinate the intricate pathophysiological functions (25–28). Intriguingly, hyper-O-GlcNAcylation of YB-1 has been reported to affect its S102 phosphorylation, and this close O-GlcNAcylation–phosphorylation interaction played indispensable roles in regulating cell proliferation and progression of hepatocellular carcinoma (28). However, a role for the phosphorylation of YB-1, which regulates its protein stability, remains unknown.

Given the role of deubiquitinase OTUB1 in regulating the ubiquitination and stability of YB-1 in renal tubular cells (10),

we aimed to investigate these roles of OTUB1–YB-1 axis in regulation of DCM. Co-IP results showed the homeostatic interaction of YB-1 and OTUB1 in cardiomyocytes, which are sensitive to diabetic microenvironment. Subsequent experiments with YB-1 mutants proved that the phosphorylation of YB-1 at S102 diminishes this homeostatic interaction with OTUB1, resulting in ubiquitination and degradation of the YB-1 *via* proteasome. Interestingly, beyond its canonical deubiquitinase activity, OTUB1 possesses a noncanonical catalytic-independent activity, in which it inhibits the transfer of ubiquitin onto protein substrates by binding to the

YB-1 phosphorylation aggravates DCM

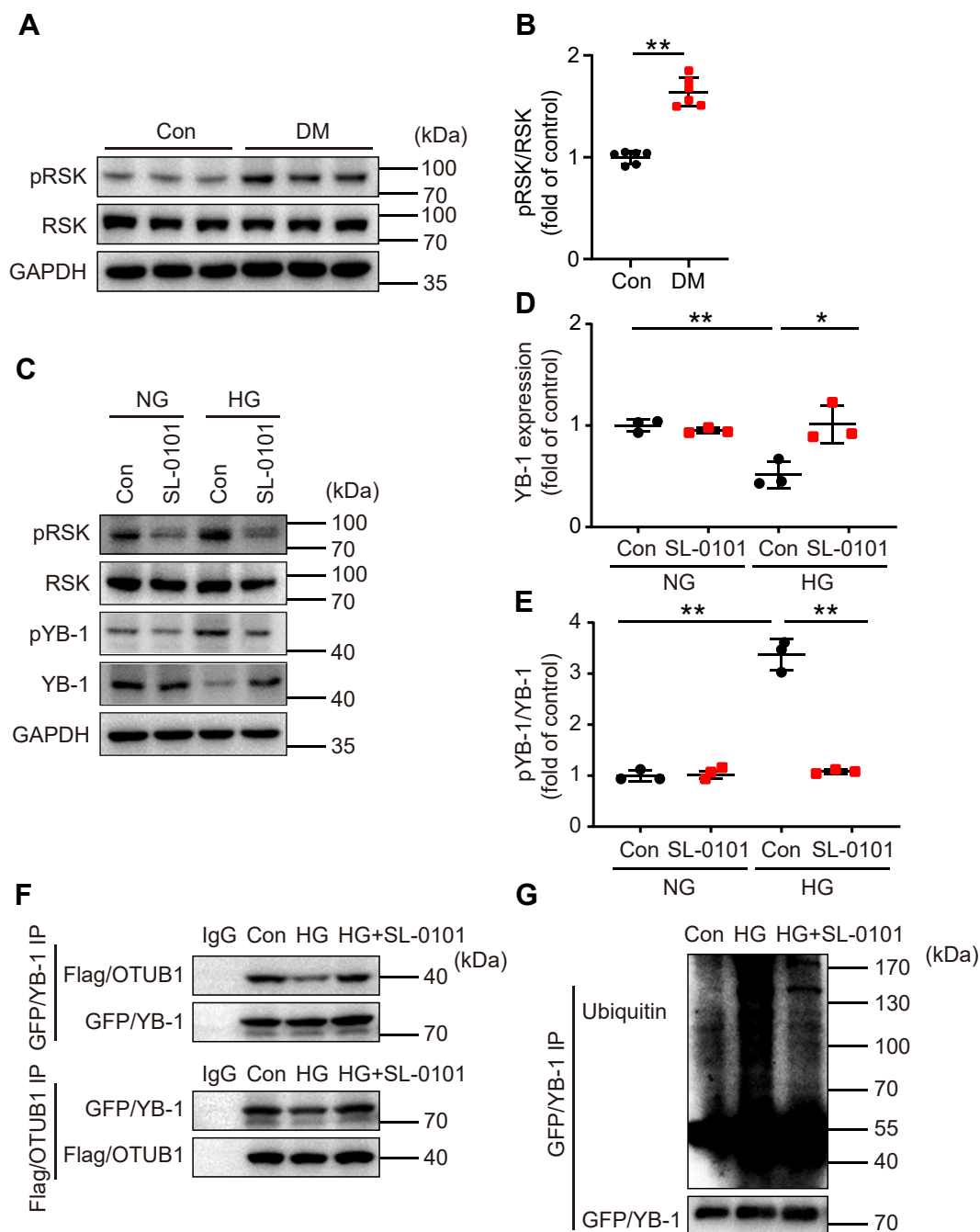


Figure 3. YB-1 phosphorylation was regulated by p90RSK. *A* and *B*, representative immunoblotting images and analyzed scatter diagram showed an increased phosphorylation of p90RSK in diabetic mice heart tissue compared with controls. *C–E*, inhibiting the activation of RSK could suppress YB-1 phosphorylation (S102) and maintain YB-1 protein level. H9c2 cells were pretreated with 100 μ M SL-0101 for 30 min and stimulated by high glucose (HG) for 24 h. *F*, SL-0101 restored the interaction between YB-1 and OTUB1, which destroyed by HG stimulation. *G*, SL-0101 ameliorated HG-induced YB-1 ubiquitination. In *B*, for each group, $n = 6$; in other panels, for each group, $n = 3$. Analyzed data are expressed as mean \pm SD. * $p < 0.05$, ** $p < 0.01$, compared with control group, Student's *t* test or One-way ANOVA, Bonferroni comparison test. DM, diabetes mellitus; NG, normal glucose; OTUB1, otubain-1; RSK, p90 ribosomal S6 kinase; S102, serine102; YB-1, Y-box binding protein-1.

ubiquitin-charged E2. Thus, OTUB1 can decrease a protein's ubiquitination state by removing ubiquitin (canonical activity) or preventing ubiquitin conjugation (noncanonical activity) (29), for example, OTUB1 can inhibit the ubiquitination of phospho-SMAD2/3 (Smad, drosophila mothers against decapentaplegic protein) by binding to and inhibiting the E2 ubiquitin-conjugating enzymes independent of its catalytic activity (30). Whether OTUB1 can regulate the ubiquitination

of YB-1 in a similar noncanonical way remains elusive. Moreover, structure biologists have recently shown that the phosphorylation of S102 disrupts the hydrogen bonding of YB-1 with the residue in the C-terminal extension, resulting in conformational changes in the regions close to S102, and in turn destabilizing its binding to its substrate single-stranded DNAs (9). Thus, it is possible that the phosphorylation of YB-1 at S102 could regulate the binding affinity of YB-1 to

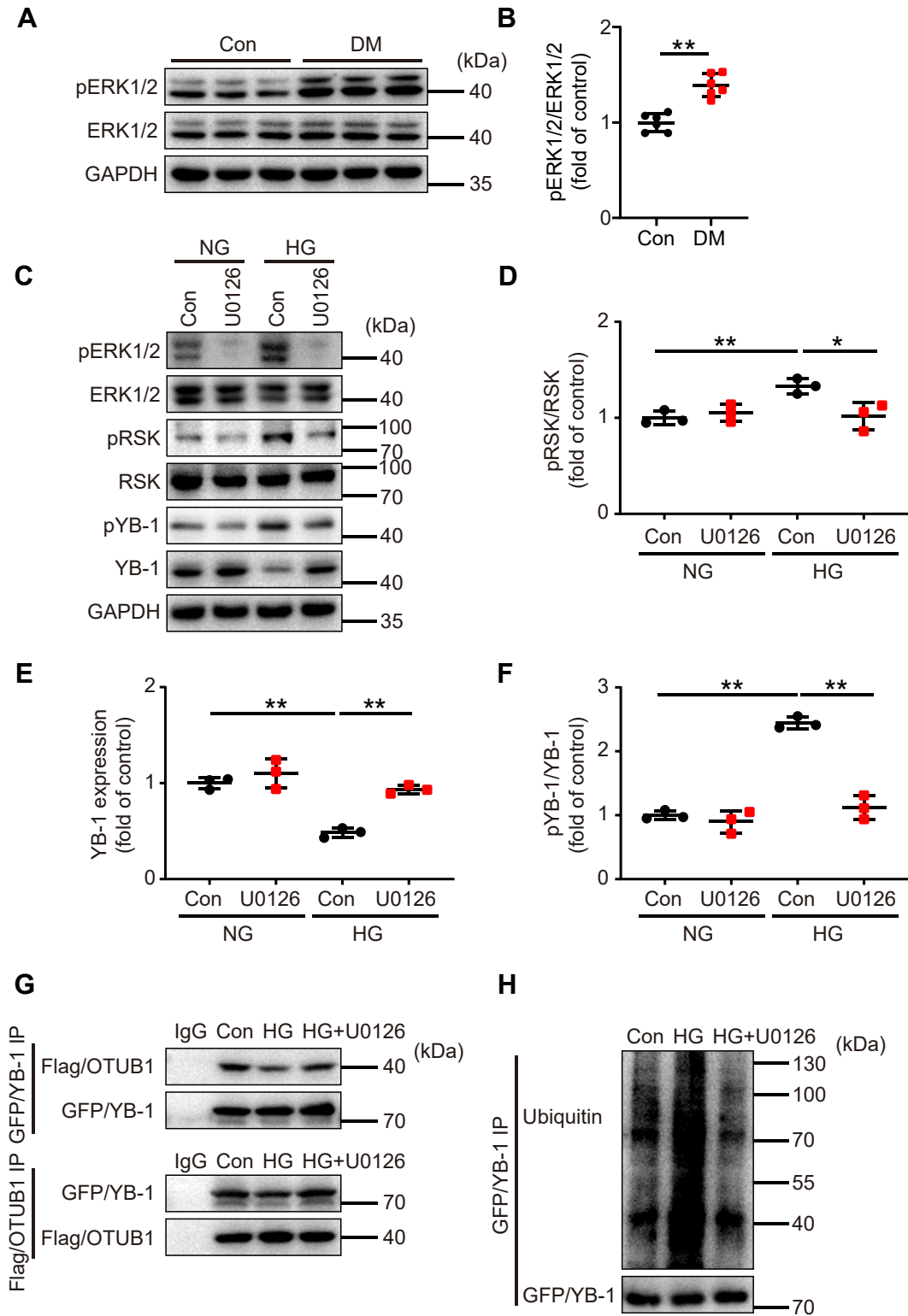


Figure 4. ERK promoted YB-1 phosphorylation. *A* and *B*, representative immunoblotting images and analyzed scatter diagram of protein expression and phosphorylation level of ERK in diabetes mellitus mice heart tissue. *C–F*, protein expression and phosphorylation level of ERK, RSK, and YB-1 in H9c2 cells interfered with high glucose (HG) and/or 10 μ M U0126. *G*, U0126 maintained the interaction between YB-1 and OTUB1. H9c2 cells were coinfected with GFP-tagged YB-1 and FLAG-tagged OTUB1-overexpressing lentivirus, pretreated with 10 μ M U0126 for 30 min, and challenged by HG for 24 h. *H*, U0126 reduced YB-1 ubiquitination modification in the context of HG stimulation. In *B*, for each group, $n = 6$; in other panels, for each group, $n = 3$. Analyzed data are expressed as mean \pm SD. * $p < 0.05$, ** $p < 0.01$, compared with control group, Student's *t* test, Bonferroni comparison test. DM, diabetes mellitus; ERK, extracellular signal-regulated kinase; NG, normal glucose; OTUB1, otubain-1; RSK, p90 ribosomal S6 kinase; YB-1, Y-box binding protein-1.

YB-1 phosphorylation aggravates DCM

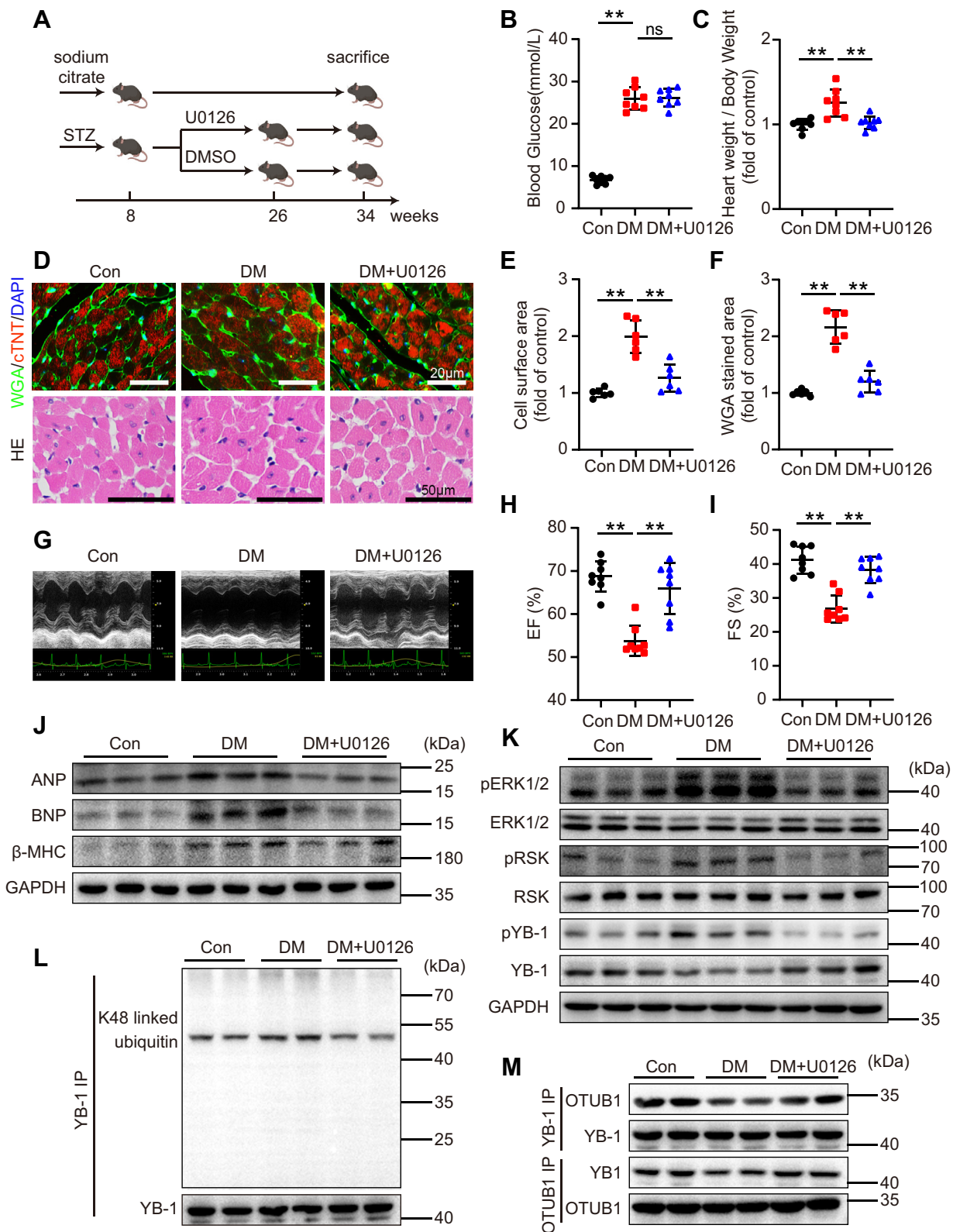


Figure 5. U0126 inhibited YB-1 phosphorylation and alleviated diabetic cardiomyopathy. *A*, animal experiment procedure. Eight-week-old male C57BL/6J mice were injected with 60 mg/kg STZ to induce diabetes mellitus, and controls received the same volume of sodium citrate. Diabetic mice were treated with 1 mg/kg U0126 or the same volume 6% DMSO in 26 weeks. All mice were sacrificed at the age of 34 weeks. *B*, blood glucose detected at 34 weeks in mice with different treatments. *C*, ratios of heart weight to body weight in mice with diverse treatments. *D*, representative histological images of transverse area of myocyte in mice with different treatments. For WGA staining, green: WGA, red: cTNT, and blue: DAPI. The scale bar represents 20 μm; for HE staining, the scale bar represents 50 μm. *E* and *F*, analyzed histological data showing the myocyte cell surface area in diabetic mice with or without U0126 treatment, relative to controls. *G*, representative echocardiography images of mice with various interventions in M mode. *H* and *I*, echocardiography analysis of EF and FS in mice with different interventions. *J*, representative immunoblotting images showing protein expression level of ANP, BNP, and β-MHC in mice heart tissue lysates. *K*, representative immunoblotting images showing protein expression and phosphorylation levels of ERK, p90RSK, and

Table 2
Echocardiography result of mice in experiment 2

Item	Con	DM	DM + U0126
Heart rate, bpm	491 ± 33.36	500 ± 33.23	494 ± 29.63
Cardiac output, ml/min	24.69 ± 4.39	15.85 ± 3.48 ^a	22.93 ± 2.62 ^b
LVAW; d, mm	0.62 ± 0.05	0.64 ± 0.07	0.60 ± 0.11
LVAW; s, mm	1.02 ± 0.06	1.03 ± 0.11	1.00 ± 0.12
LVID; d, mm	4.68 ± 0.43	4.13 ± 0.26 ^a	4.55 ± 0.21 ^b
LVID; s, mm	3.56 ± 0.55	3.07 ± 0.44	3.47 ± 0.46
LVPW; d, mm	0.63 ± 0.05	0.61 ± 0.09	0.61 ± 0.10
LVPW; s, mm	0.98 ± 0.08	0.91 ± 0.13	0.99 ± 0.12

Data are presented as mean ± SD, n = 8.

^a *p* < 0.01 versus Con.

^b *p* < 0.01 versus Con.

Abbreviations: DM, diabetes mellitus; LVAW, left ventricular anterior wall; LVID, left ventricular internal dimension; LVPW, left ventricular posterior wall.

OTUB1 through conformational changes as well (9). The last but not the least, whether hyperglycemia can alter the expression or stability of OTUB1 itself and then that of YB-1 requires further elucidation.

Protein kinase B (AKT) (31, 32), p90 S6 ribosomal kinase (RSK) (33), and ERK (34, 35) have all been implicated in YB-1 S102 phosphorylation. The current study showed that the phosphorylation of AKT at T308 and S473 was downregulated in diabetic heart and high glucose-treated cardiomyocytes. However, blocking the phosphorylation with specific inhibitors resulted in no significant impact on S102 phosphorylation of YB-1 in cardiomyocyte. This discrepancy indicates that the effect of AKT on S102 phosphorylation of YB-1 could be cell type and context dependent. Whereas ERK inhibitor U0126 and RSK inhibitor SL-0101 worked as we presumed, and ERK seems to be upstream signaling intermediate of RSK (36–39). RSK inhibitor SL-0101 and its analog have been so far only tested in two studies in mouse models *in vivo*, one in triple-negative breast cancer metastasis (40) and the other one in Herpes simplex virus-1 infection (41). Moreover, SL-0101 has been shown to induce distinct off-target effects in mammalian target of rapamycin complex 1–p70S6K signaling pathway. While ERK inhibitor U0126 has been widely used for ERK1/2 inhibition *in vivo* and has little side effects *in vivo* as reported by Miyoshi *et al.* (42). Besides, another study has reported that inhibition of ERK but not RSK efficiently suppresses the epidermal growth factor receptor reporter activity *via* YB-1 S102 phosphorylation. Hence, we employed the ERK inhibitor U0126 for the *in vivo* experiment. Indeed, U0126 could ameliorate DCM indices when compared with the vehicle-treated diabetic mice. In accordance with our *in vitro* findings, U0126 could suppress the ERK phosphorylation, RSK phosphorylation, and subsequent YB-1 S102 phosphorylation, resulting in enhanced interaction between YB-1 and OTUB1 and preserved YB-1 protein expression in diabetic hearts. Recently, we showed that the YB-1 acts as a transcriptional suppressor, which binds directly to the promoter region of

another important cardiomyopathy-related transcriptional factor myocyte enhancer factor 2B and suppresses its expression. Hyperglycemia caused proteasome-dependent YB-1 protein degradation results in myocyte enhancer factor 2B overexpression, which contributes to the development and formation of DCM (43).

In conclusion, phosphorylation of YB-1 on S102 *via* ERK/RSK pathway under hyperglycemia condition could impair its interaction with deubiquitinase OTUB1, leading to enhanced YB-1 K48 ubiquitination and its subsequent degradation *via* proteasome in diabetic heart. Targeting ERK/RSK/YB-1 pathway could be a potential therapeutic approach for DCM.

Experimental procedures

Experimental animals and study design

The research was approved by the Institutional Animal Research Committee of Tongji Medical College. Six-week-old C57BL/6J male mice were purchased from HFK Bioscience and housed in the specific pathogen-free animal care facility of Tongji Medical College Experimental Animal Center. All animal procedures were carried out in compliance with the Directive 2010/63/EU of the European Parliament on the protection of animals used for scientific purposes, the requirements of the local Institutional Animal Research Committee, and the ARRIVE (Animal Research: Reporting of In Vivo Experiments) guidelines.

For the purpose of investigating YB-1 phosphorylation regulation in DCM, type 1 diabetes mellitus animal model was induced by intraperitoneal injection of STZ (Sigma–Aldrich). Briefly, 8-week-old male C57BL/6J mice received 60 mg/kg STZ for 5 consecutive days to establish diabetes mellitus or the equal volume of sterilized pH 4.5, 0.05 M sodium citrate solution to serve as control (n = 8 for each group).

For the purpose of evaluating the effect of MEK inhibitor U0126 on DCM, diabetic mice (at 18 weeks post STZ intervention) were treated daily with 1 mg/kg U0126 (LC

YB-1 in mice treated with or without U0126, compared with controls. *L*, YB-1 immunoprecipitation in mice heart tissue lysates showing the impact of U0126 treatment on K48-linked ubiquitination of YB-1. *M*, interaction between YB-1 and OTUB1 detected by immunoprecipitation of YB-1 and OTUB1, respectively, in different group of mice heart tissue lysates. For all groups, n = 8. Data are expressed as mean ± SD. ***p* < 0.01; ns, One-way ANOVA, Bonferroni comparison test. ANP, atrial natriuretic peptide; BNP, brain natriuretic peptide; cTNT, cardiac troponin T; DAPI, 4',6-diamidino-2-phenylindole; DM, diabetes mellitus; DMSO, dimethyl sulfoxide; EF, ejection fraction; ERK, extracellular signal-regulated kinase; FS, fraction shortening; K48, lysine 48; β-MHC, β-myosin heavy chain; ns, not significant; OTUB1, otubain-1; RSK, p90 ribosomal S6 kinase; STZ, streptozotocin; WGA, wheat germ agglutinin; YB-1, Y-box binding protein-1.

YB-1 phosphorylation aggravates DCM

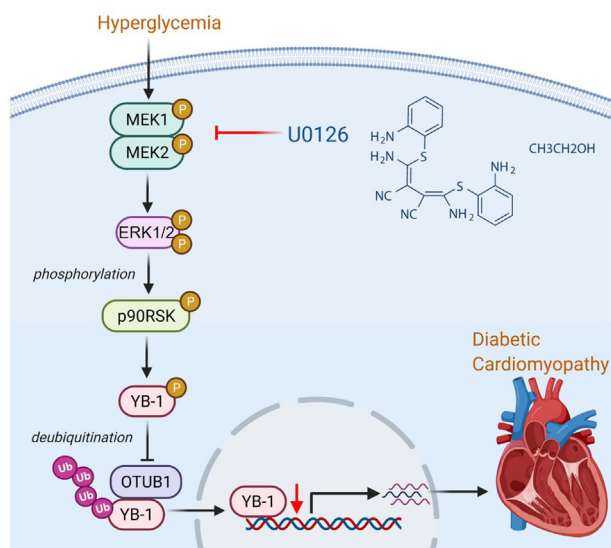


Figure 6. Graphical abstract. Hyperglycemia increased the MEK1/2 phosphorylation, leading to the significant elevation of the ERK1/2 phosphorylation, which in turn induces the p90RSK phosphorylation. Thereafter, the YB-1 phosphorylation (S102) was promoted by the p90RSK, and the interaction between OTUB1 and YB-1 was subsequently suppressed, resulting in the YB-1 protein ubiquitination and degradation via the proteasome. The diminished YB-1 protein level altered the transcription of related target genes and contributing to the occurrence and progression of diabetic cardiomyopathy. Pharmacological inhibition of the ERK pathway using the MEK inhibitor U0126 could relieve the process described previously, thus alleviating diabetic cardiomyopathy. ERK, extracellular signal-regulated kinase; MEK, mitogen-activated protein kinase; OTUB1, otubain-1; RSK, p90 ribosomal S6 kinase; S102, serine102; YB-1, Y-box binding protein-1.

Laboratories) or the same volume of 6% dimethyl sulfoxide–PBS for 8 weeks ($n = 8$ for all groups).

Body weight and blood glucose were monitored continuously after the STZ administration. There was no mortality related to diabetes during the progression of DCM. Insulin Lantus (Sanofi) was administered subcutaneously when blood glucose went higher than 27.7 mmol/L. All animals were sacrificed at the age of 34 weeks with excessive xylazine and ketamine mixture. Blood and heart were subsequently harvested.

Echocardiography and hemodynamic analysis

Echocardiography analysis was performed by ultrasound professionals with a 30-MHz high-frequency scan head (VisualSonics Vevo770; VisualSonics) in M mode. Images were analyzed by the VevoLab software (VisualSonics). Hemodynamic parameters were recorded by inserting a Millar Catheter (Millar 1.4F, SPR835; Millar Instruments, Inc) into the left ventricle *via* right carotid artery. Data analysis was performed with the PVAN software (Millar Instruments, Inc).

Histological and immunohistochemical staining

Mice heart tissues were flushed with ice-cold PBS thoroughly after sacrifice and divided into several parts. Left ventricles were fixed with 4% paraformaldehyde (ServiceBio) for 48 h, embedded in paraffin, and cut into serial 4 μ m sections. HE staining (Jiancheng) and WGA staining (Sigma–Aldrich), which combined with immunofluorescence staining of cardiac

troponin T (15513-1-AP; Proteintech Group) and 4',6-diamidino-2-phenylindole (Beyotime), were used to analyze the morphology of cardiomyocytes and quantify transverse cardiomyocyte size. For immunohistochemical staining of mice heart tissues, we used primary antibodies against phosphorylated YB-1 (CSB-PA204680; CUSABIO), YB-1 (ab76149; Abcam), and phosphorylated ERK (No. 4376; Cell Signaling Technology). The isotype antibody was used as negative control. Corresponding horseradish peroxidase–conjugated secondary antibodies (ServiceBio) and DAB (Vector Laboratories) were used for detection. Images were captured by microscopes (Olympus) and analyzed by Image-Pro Plus software (X-ray Scan).

Plasmid construction

The ORF of YB-1 was amplified by PCR (primer sequence, forward: ATGAGCAGCGAGGCCGA, reverse: TTACTIONA GCCCGCCCTG) and inserted into the pEGFP-C1 vector. The EGFP-YB-1 DNA fragment was cut down by *Nhe*I and *Xba*I endonuclease (New England Biolabs) and inserted into the lentiviral vector FuGW (No. 14883; Addgene) by T4 ligase (New England Biolabs). To regulate the phosphorylation state of YB-1, two point mutations were introduced to convert the S102-encoding AGT to CGT or GAT encoding for alanine (102A) or aspartic acid (102D) with QuickMutation Plus Site-Directed Mutagenesis Kit (D0208; Beyotime), according to the manufacturer's protocol.

Cell culture

H9c2 cells (American Type Culture Collection) were cultured in Dulbecco's modified Eagle's medium containing 1.5 g/L glucose with 10% fetal bovine serum (Gibco, Thermo Fisher Scientific). To imitate hyperglycemia, 25 mmol/L glucose (Sigma–Aldrich) was used to stimulate H9c2 cells, and 25 mmol/L mannitol was used as control. To explore which signaling pathway(s) participated in the regulation of YB-1 phosphorylation in DCM, H9c2 cells were pretreated with different pharmacological blockades for 30 min, including U0126, SL-0101 (MedChemExpress), or MK2206 (Selleck), and then coincubated with high glucose for 24 h.

IP and immunoblotting

Protein extraction was performed with radioimmunoprecipitation assay buffer (50 mM Tris at pH 7.4, 1% NP-40, 0.25% sodium deoxycholate, 150 mM NaCl, 1 mM EDTA, and 1 mM Na_3VO_4) in heart tissues and with cell lysis buffer for Western and IP (P0013; Beyotime) in H9c2 cells, both supplemented with protease and phosphatase inhibitor cocktails (HY-K0010, HY-K0021; MedChemExpress). Lysates were centrifuged at 12,000g for 25 min at 4 °C, and supernatants were collected and quantified with bicinchoninic acid reagents (Boster).

To perform IP in heart tissue, lysates were first incubated with 20 μ l protein A/G agarose beads (Santa Cruz) for 30 min to eliminate nonspecific binding. Then, supernatants were collected and incubated with 1 μ g antibody to YB-1 (ab76149; Abcam) or OTUB1 (No. 3783; Cell Signaling Technology) for

1 h. Protein A/G agarose beads were employed to precipitate the antigen–antibody complex at 4 °C overnight and collected for Western blot detection.

To investigate the effect of different interventions on ubiquitination modification of YB-1, H9c2 cells were infected with GFP-tagged YB-1-overexpressing lentivirus for 48 h. During the expression period, H9c2 cells received interventions described in cell culture. In experiments of verifying the effect of YB-1 phosphorylation on YB-1 ubiquitination, H9c2 cells were infected with GFP-tagged YB-1 WT lentivirus or YB-1 102A and 102D mutant lentivirus to imitate inactivation or activation state of YB-1 phosphorylation. To explore the interaction between YB-1 and OTUB1, H9c2 cells were coinfecting with GFP-tagged YB-1 and FLAG-tagged OTUB1 overexpressing lentivirus for 48 h and also received different interventions described previously. Then, we standardized the total amount of GFP-YB-1 protein or FLAG-OTUB1 protein used for IP or co-IP separately with their corresponding input control and precipitated them with 1 µg anti-GFP or anti-FLAG primary antibody (Nos. 2955 and 14793; Cell Signaling Technology). Isotype antibody was used as negative control. Finally, we used Western blot to evaluate the YB-1 ubiquitination and the integrated OTUB1 level while YB-1 was served as loading control, and vice versa.

Protein lysates and IP complex were used for electrophoresis, transferred to 0.45 µm polyvinylidene difluoride membranes, blocked with 5% bovine serum albumin, and incubated with primary antibodies overnight. The following antibodies were used: ANP, BNP, β-MHC, p90RSK, phospho-p90RSK (Nos. A14755, A2172, A7564, A15718, AP0539; Abclonal), phosphorylated YB-1 and YB-1 (CSB-PA204680, CSB-PA020158; CUSABIO), ERK, phosphorylated ERK, OTUB1, ubiquitin, K48-linkage specific polyubiquitin, GFP, FLAG (Nos. 4695, 4376, 3783, 3936, 4289, 2955, and 14793; Cell Signaling Technology), GAPDH (GB11002; ServiceBio), and horseradish peroxidase–conjugated secondary antibodies (ServiceBio).

Statistics and reproducibility

Statistical analysis was performed with SPSS 24.0 software (IBM Corp). Data were expressed as mean ± SD. Statistical significance was defined as *p* value <0.05, and normality was assessed using the Shapiro–Wilk test. Differences between the two groups were evaluated by unpaired Student's *t* test. In case of significant interaction between groups, comparisons between three or more groups were further conducted within each group using ANOVA, with Bonferroni post hoc test.

Data availability

The data underlying this article are available in the article and in its online supporting material.

Supporting information—This article contains supporting information.

Acknowledgments—We thank Zheng Wen for her valuable technical support with echocardiography.

Author contributions—H. W. conceptualization; X. Z., T. W., and M. W. methodology; T. W., M. W., and L. D. validation; X. Z. formal analysis; X. Z. investigation; H. Z. resources; W. Z. and Y. X. data curation; X. Z. writing—original draft; H. W. and T. M. writing—review & editing; W. Z. and Y. X. visualization; H. Z. supervision; X. H. project administration; H. Z. and X. H. funding acquisition.

Funding and additional information—This work was supported by the National Natural Science Foundation of China (grant Nos.: 81600301 [to H. W.]; 81873523 and 82070490 [to H. Z.]; and 81800411 [to X. H.]) and Medicine and Health Science Technology Development Program of Shandong Province (grant No.: 2018WS050 [to T. W.]).

Conflict of interest—H. W. reports that financial support was provided by the National Natural Science Foundation of China. H. Z. reports that financial support was provided by the National Natural Science Foundation of China. X. H. reports that financial support was provided by the National Natural Science Foundation of China. T. W. reports that financial support was provided by the Medicine and Health Science Technology Development Program of Shandong Province. All other authors declare that they have no conflicts of interest with the contents of this article.

Abbreviations—The abbreviations used are: ANP, atrial natriuretic peptide; BNP, brain natriuretic peptide; co-IP, coimmunoprecipitation; DCM, diabetic cardiomyopathy; ERK, extracellular signal-regulated kinase; K48, lysine 48; MEK, mitogen-activated protein kinase; β-MHC, β-myosin heavy chain; OUT, ovarian tumor domain; OTUB1, otubain-1; PTM, post-translational modification; RSK, p90 S6 ribosomal kinase; S102, serine102; STZ, streptozotocin; WGA, wheat germ agglutinin; YB-1, Y-box binding protein-1.

References

- Rubler, S., Dlugash, J., Yuçoglu, Y. Z., Kumral, T., Branwood, A. W., and Grishman, A. (1972) New type of cardiomyopathy associated with diabetic glomerulosclerosis. *Am. J. Cardiol.* **30**, 595–602
- Ritchie, R. H., and Abel, E. D. (2020) Basic mechanisms of diabetic heart disease. *Circ. Res.* **126**, 1501–1525
- Jia, G., Hill, M. A., and Sowers, J. R. (2018) Diabetic cardiomyopathy: an update of mechanisms contributing to this clinical entity. *Circ. Res.* **122**, 624–638
- Udell, J. A., Cavender, M. A., Bhatt, D. L., Chatterjee, S., Farkouh, M. E., and Scirica, B. M. (2015) Glucose-lowering drugs or strategies and cardiovascular outcomes in patients with or at risk for type 2 diabetes: a meta-analysis of randomised controlled trials. *The Lancet. Diabetes Endocrinol.* **3**, 356–366
- Reaven, P. D., Emanuele, N. V., Wiitala, W. L., Bahn, G. D., Reda, D. J., McCarren, M., et al. (2019) Intensive glucose control in patients with type 2 diabetes - 15-year follow-up. *New Engl. J. Med.* **380**, 2215–2224
- Lindquist, J. A., and Mertens, P. R. (2018) Cold shock proteins: from cellular mechanisms to pathophysiology and disease. *Cell Commun. Signal.* **16**, 63
- Mordovkina, D., Lyabin, D. N., Smolin, E. A., Sogorina, E. M., Ovchinnikov, L. P., and Eliseeva, I. (2020) Y-box binding proteins in mRNP assembly, translation, and stability control. *Biomolecules* **10**, 591
- Budkina, K. S., Zlobin, N. E., Kononova, S. V., Ovchinnikov, L. P., and Babakov, A. V. (2020) Cold shock domain proteins: structure and interaction with nucleic acids. *Biochemistry. Biokhimiia* **85**, S1–S19
- Zhang, J., Fan, J., Li, S., Yang, Y., Sun, P., Zhu, Q., et al. (2020) Structural basis of DNA binding to human YB-1 cold shock domain regulated by phosphorylation. *Nucl. Acids Res.* **48**, 9361–9371

YB-1 phosphorylation aggravates DCM

- Dong, W., Wang, H., Shahzad, K., Bock, F., Al-Dabet, M. M., Ranjan, S., et al. (2015) Activated protein C ameliorates renal ischemia-reperfusion injury by restricting Y-box binding protein-1 ubiquitination. *J. Am. Soc. Nephrol.* **26**, 2789–2799
- Cao, X., Zhu, N., Zhang, Y., Chen, Y., Zhang, J., Li, J., et al. (2020) Y-box protein 1 promotes hypoxia/reoxygenation- or ischemia/reperfusion-induced cardiomyocyte apoptosis via SHP-1-dependent STAT3 inactivation. *J. Cell Physiol.* **235**, 8187–8198
- Kamalov, G., Varma, B. R., Lu, L., Sun, Y., Weber, K. T., and Guntaka, R. V. (2005) Expression of the multifunctional Y-box protein, YB-1, in myofibroblasts of the infarcted rat heart. *Biochem. Biophys. Res. Commun.* **334**, 239–244
- Choong, O. K., Chen, C., Zhang, J., Lin, J., Lin, P., Ruan, S., et al. (2019) Hypoxia-induced H19/YB-1 cascade modulates cardiac remodeling after infarction. *Theranostics* **9**, 6550–6567
- David, J. J., Subramanian, S. V., Zhang, A., Willis, W. L., Kelm, R. J., Leier, C. V., et al. (2012) Y-box binding protein-1 implicated in translational control of fetal myocardial gene expression after cardiac transplant. *Exp. Biol. Med.* **237**, 593–607
- Gao, D., Niu, Q., Gong, Y., Guo, Q., Zhang, S., Wang, Y., et al. (2021) Y-box binding protein 1 regulates angiogenesis in bladder cancer via miR-29b-3p-VEGFA pathway. *J. Oncol.* **2021**, 9913015
- Xue, X., Huang, J., Yu, K., Chen, X., He, Y., Qi, D., et al. (2020) YB-1 transferred by gastric cancer exosomes promotes angiogenesis via enhancing the expression of angiogenic factors in vascular endothelial cells. *BMC Cancer* **20**, 996
- Juang, Y., Landry, M., Sanches, M., Vittal, V., Leung, C. C. Y., Ceccarelli, D. F., et al. (2012) OTUB1 co-opts Lys48-linked ubiquitin recognition to suppress E2 enzyme function. *Mol. Cell* **45**, 384–397
- Sivakumar, D., Kumar, V., Naumann, M., and Stein, M. (2020) Activation and selectivity of OTUB-1 and OTUB-2 deubiquitinylases. *J. Biol. Chem.* **295**, 6972–6982
- Edelmann, M. J., Iphöfer, A., Akutsu, M., Altun, M., di Gleria, K., Kramer, H. B., et al. (2009) Structural basis and specificity of human otubain 1-mediated deubiquitination. *Biochem. J.* **418**, 379–390
- Saldana, M., VanderVorst, K., Berg, A. L., Lee, H., and Carraway, K. L. (2019) Otubain 1: a non-canonical deubiquitinase with an emerging role in cancer. *Endocr-Relat Cancer* **26**, R1–R14
- Suresh, P. S., Tsutsumi, R., and Venkatesh, T. (2018) YBX1 at the crossroads of non-coding transcriptome, exosomal, and cytoplasmic granular signaling. *Eur. J. Cell Biol.* **97**, 163–167
- Prabhu, L., Hartley, A., Martin, M., Warsame, F., Sun, E., and Lu, T. (2015) Role of post-translational modification of the Y box binding protein 1 in human cancers. *Genes Dis.* **2**, 240–246
- Martin, M., Hua, L., Wang, B., Wei, H., Prabhu, L., Hartley, A., et al. (2017) Novel serine 176 phosphorylation of YBX1 activates NF- κ B in colon cancer. *J. Biol. Chem.* **292**, 3433–3444
- Mehta, S., Algie, M., Al-Jabry, T., McKinney, C., Kannan, S., Verma, C. S., et al. (2020) Critical role for cold shock protein YB-1 in cytokinesis. *Cancers* **12**, 2473
- Tao, W., Jinhua, W., Wei, D., Mengwen, W., Xiaodan, Z., Wenjun, Z., et al. (2021) The MEK inhibitor U0126 ameliorates diabetic cardiomyopathy by restricting XBP1's phosphorylation dependent SUMOylation. *Int. J. Biol. Sci.* **12**, 2984–2999
- Nie, Q., Gong, X., Liu, M., and Li, D. W. (2017) Effects of crosstalks between sumoylation and phosphorylation in normal cellular physiology and human diseases. *Curr. Mol. Med.* **16**, 906–913
- Yao, Q., Li, H., Liu, B., Huang, X., and Guo, L. (2011) SUMOylation-regulated protein phosphorylation, evidence from quantitative phosphoproteomics analyses. *J. Biol. Chem.* **286**, 27342–27349
- Liu, Q., Tao, T., Liu, F., Ni, R., Lu, C., and Shen, A. (2016) Hyper-O-GlcNAcylation of YB-1 affects Ser102 phosphorylation and promotes cell proliferation in hepatocellular carcinoma. *Exp. Cell Res.* **349**, 230–238
- Zhu, Q., Fu, Y., Li, L., Liu, C. H., and Zhang, L. (2021) The functions and regulation of Otubains in protein homeostasis and diseases. *Ageing Res. Rev.* **67**, 101303
- Herhaus, L., Al-Salihi, M., Macartney, T., Weidlich, S., and Sapkota, G. P. (2013) OTUB1 enhances TGF β signalling by inhibiting the ubiquitylation and degradation of active SMAD2/3. *Nat. Commun.* **4**, 2519
- Sutherland, B. W., Kucab, J., Wu, J., Lee, C., Cheang, M. C. U., Yorida, E., et al. (2005) Akt phosphorylates the Y-box binding protein 1 at Ser102 located in the cold shock domain and affects the anchorage-independent growth of breast cancer cells. *Oncogene* **24**, 4281–4292
- Liao, L., Chen, C., Li, N., Lin, L., Huang, B., Chang, Y., et al. (2020) Y-box binding protein-1 promotes epithelial-mesenchymal transition in sorafenib-resistant hepatocellular carcinoma cells. *Int. J. Mol. Sci.* **22**, 224
- Sechi, M., Lall, R. K., Afolabi, S. O., Singh, A., Joshi, D. C., Chiu, S., et al. (2018) Fisetin targets YB-1/RSK axis independent of its effect on ERK signaling: Insights from *in vitro* and *in vivo* melanoma models. *Sci. Rep-uk* **8**, 15726
- Toulany, M., Schickfluss, T., Eicheler, W., Kehlbach, R., Schittek, B., and Rodemann, H. P. (2011) Impact of oncogenic K-RAS on YB-1 phosphorylation induced by ionizing radiation. *Breast Cancer Res.* **13**, R28
- Tiwari, A., Iida, M., Kosnopfel, C., Abbariki, M., Menegakis, A., Fehrenbacher, B., et al. (2020) Blocking Y-box binding protein-1 through simultaneous targeting of PI3K and MAPK in triple negative breast cancers. *Cancers* **12**, 2795
- Smith, J. A., Poteet-Smith, C. E., Xu, Y., Errington, T. M., Hecht, S. M., and Lannigan, D. A. (2005) Identification of the first specific inhibitor of p90 ribosomal S6 kinase (RSK) reveals an unexpected role for RSK in cancer cell proliferation. *Cancer Res.* **65**, 1027–1034
- Stratford, A. L., Fry, C. J., Desilets, C., Davies, A. H., Cho, Y. Y., Li, Y., et al. (2008) Y-box binding protein-1 serine 102 is a downstream target of p90 ribosomal S6 kinase in basal-like breast cancer cells. *Breast Cancer Res.* **10**, R99
- Roffé, M., Lupinacci, F. C., Soares, L. C., Hajj, G. N., and Martins, V. R. (2015) Two widely used RSK inhibitors, BI-d1870 and SL0101, alter mTORC1 signaling in a RSK-independent manner. *Cell. Signal.* **27**, 1630–1642
- Tiwari, A., Rebholz, S., Maier, E., Dehghan Harati, M., Zips, D., Sers, C., et al. (2018) Stress-induced phosphorylation of nuclear YB-1 depends on nuclear trafficking of p90 ribosomal S6 kinase. *Int. J. Mol. Sci.* **19**, 2441
- Ludwik, K. A., Campbell, J. P., Li, M., Li, Y., Sandusky, Z. M., Pasic, L., et al. (2016) Development of a RSK inhibitor as a novel therapy for triple-negative breast cancer. *Mol. Cancer Ther.* **15**, 2598–2608
- Ding, X., Krutzik, P. O., Ghaffari, A. A., Zhaozhi, Y., Miranda, D. J., Cheng, G., et al. (2019) Cellular signaling analysis shows antiviral, ribavirin-mediated ribosomal signaling modulation. *Antivir. Res.* **171**, 104598
- Miyoshi, S., Hamada, H., Hamaguchi, N., Kato, A., Katayama, H., Irifune, K., et al. (2012) Antitumor activity of MEK and PI3K inhibitors against malignant pleural mesothelioma cells *in vitro* and *in vivo*. *Int. J. Oncol.* **41**, 449–456
- Zhong, X., Wang, T., Xie, Y., Wang, M., Zhang, W., Dai, L., et al. (2021) Activated protein C ameliorates diabetic cardiomyopathy via modulating OTUB1/YB-1/MEF2B axis. *Front. Cardiovasc. Med.* **8**, 758158